14th International Symposium on Turbulence and Shear Flow Phenomena (TSFP14)
Heidelberg, Germany, July 28-31, 2026

MORPHOLOGY-BASED CNN RECOGNITION OF TRANSITIONAL STATES ON FINITE CYLINDER

Yu-Hsiang Chen
Department of Aeronautics and Astronautics
National Cheng Kung University
Tainan, Taiwan 70101
pt8643631@gmail.com

Jiun-Jih Miau
Department of Aeronautics and Astronautics
National Cheng Kung University
Tainan, Taiwan 70101
jjmiau@mail.ncku.edu.tw

Yng-Ru Chen
Department of Aeronautics and Astronautics
National Cheng Kung University
Tainan, Taiwan 70101
yngru.chen@gmail.com

ABSTRACT

This study presents a morphology-based convolutional neural network (CNN) framework for identifying transitional pressure-signal states over a finite circular cylinder in the critical Reynolds-number regime. The framework segments pressure signals into 200-ms windows and converts each segment into standardized images for classification. The segments are categorized into four representative waveform families: stable flow (ST), pulse-type excursions (Pulse), transitional plateau (TP), and sustained plateau (SP), or labeled as unidentified if the classification confidence is low.

The proposed framework achieves an overall F1 score of approximately 0.94 for the four canonical waveform families. The resulting morphology statistics reveal clear spanwise differences in the transition pathway. Near the cylinder base (z/D = 1), the signal composition evolves progressively from ST-dominated behavior to Pulse-rich activity, followed by TP and finally SP dominance. In contrast, the mid-span region (z/D = 2) exhibits a narrower transition range and a less distinct TP stage, suggesting a more abrupt progression toward SP-dominated behavior. Post hoc analysis further shows that the unidentified samples are not randomly distributed residuals but form structured groups in feature space. These findings indicate that the proposed framework is effective for organizing spanwise variations in transitional pressure-signal morphology over the finite cylinder.

INTRODUCTION

The complexity of the flow over a finite-height circular cylinder exceeds that of a two-dimensional cylinder. This increased complexity stems from the simultaneous impact of ground-induced, sidewall, and free-end effects on the wake (Kawamura et al., 1984). Beyond lateral shear layers and wake vortices, the flow is influenced by a horseshoe vortex system at the base and strong downwash with tip-related vortices at the free end (Krajnović, 2011; Sumner, 2013). These interacting structures create a highly three-dimensional, spanwise non-uniform organization of the surface flow and wake.

In the critical transition regime, this complexity is further amplified by the deformation and asymmetric development of separation-bubbles, causing local pressure signals to exhibit diverse waveform morphologies rather than a single isolated mode (Lai and Miau, 2021; Lai et al., 2023). Consequently, different heights and circumferential locations may undergo different transition stages simultaneously, making the finite-cylinder wake a challenging environment for signal-based flow interpretation.

Conventional analyses of transitional pressure signals have frequently relied on threshold-based criteria to identify specific events or regimes (Veerasamy and Atkin, 2020; Zhang et al., 1996). While effective for strong, well-isolated signatures, these methods are inherently sensitive to the choice of cutoff values. Strict thresholds may overlook weak or partially developed signatures, whereas loose thresholds can misinterpret background fluctuations as physically meaningful events. Consequently, threshold-based methods are often case-dependent and may not capture the full morphological diversity of transitional waveforms, particularly when canonical states coexist with intermediate or hybrid signatures. Given that local flow organization in finite-cylinder wakes varies significantly with Reynolds number and position, a shape-oriented diagnostic framework is more desirable.

To address this issue, the present study adopts a morphology-based classification framework that emphasizes waveform shape rather than direct amplitude thresholding. Pressure time series measured on a finite circular cylinder are segmented into physics-informed 200-ms windows and transformed into standardized waveform images within a fixed pressure-coefficient range. These waveform images are then classified by a convolutional neural network (CNN) into four representative waveform families (Cheng et al., 2024; Wen et al., 2023): stable flow (ST), pulse-type excursions (Pulse), transitional plateau (TP), and sustained plateau (SP). In addition, a confidence-based unidentified category is introduced to retain segments that do not conform clearly to any of the four main waveform families (Ni et al., 2019). This design allows the framework not only to organize the dominant waveform patterns, but also to preserve intermediate, mixed, and non-canonical signatures for further physical interpretation.

The objective of this work is twofold. First, it establishes a morphology-based recognition framework for classifying transitional pressure signals over a finite circular cylinder into four representative waveform families while retaining low-confidence samples through a rejection mechanism. Second, it uses the resulting classification maps to examine how waveform composition varies with spanwise position and Reynolds number, with particular attention to the contrast between the base and middle parts of the cylinder and to the role of unidentified samples in indicating structured intermediate waveform behavior. In this sense, the present work focuses primarily on signal-based organization of transitional states, rather than on a one-to-one identification of individual flow structures.

EXPERIMENTAL SETUP AND DATASET

The experimental data used in the present study were obtained from surface-pressure measurements on a smooth finite circular cylinder with an aspect ratio of 4. The experiments were conducted in the open-type wind tunnel at National Cheng Kung University. Pressure signals were measured from twelve miniature pressure taps distributed over three spanwise locations, z/D = 1, 2, and 3.5, and four azimuthal positions, $\theta = \pm 90°$ and $\pm 110°$. This arrangement allows the present analysis to capture both circumferential and spanwise variations in local surface-pressure behavior, thereby providing a basis for examining the three-dimensional organization of transitional waveform states over the finite cylinder. The Reynolds number range considered in this study extends from 2.1×10^5 to 3.5×10^5, covering the critical transition regime in which stable, pulse-like, and plateau-type waveform morphologies coexist. Within this range, the surface flow undergoes substantial reorganization, and the associated pressure signals often display strong intermittency and local variability. To facilitate consistent morphological analysis across different Reynolds numbers and measurement locations, each continuous pressure record was divided into fixed 200-ms segments. This window length was chosen to be on the order of two dominant vortex-shedding periods, so that each segment retains sufficient temporal context to represent a waveform morphology while remaining short enough to preserve sensitivity to rapid state changes.

For subsequent image-based processing, each segment was plotted within a fixed pressure-coefficient window spanning Cp = 0 to -3.0. The resulting waveform plots were converted into grayscale images with a resolution of 128 × 128 pixels. By representing all waveform segments in a common image frame, the analysis emphasizes differences in global waveform morphology under a consistent reference scale. The same dataset was then used to construct classification maps as functions of spanwise location and Reynolds number. These maps provide the basis for examining how local waveform morphology evolves across the finite cylinder within the transitional Reynolds-number range.

MORPHOLOGY-BASED CLASSIFICATION

Canonical Waveform Categories

To characterize the diverse pressure-signal behaviors observed over the finite circular cylinder in the transitional Reynolds-number range, the present study adopts a morphology-based classification framework built upon four representative waveform families: ST, Pulse, TP, and SP. These waveform families are introduced as canonical morphology references for organizing the dominant pressure-signal patterns in the dataset. Rather than relying solely on scalar descriptors such as peak value, mean pressure, or fluctuation intensity, the present framework emphasizes the overall waveform shape within a fixed time window.

As illustrated in Figure 1, the ST family corresponds to waveform segments in which the pressure signal remains near a relatively stable baseline without pronounced impulsive excursions or persistent low-pressure plateaus. In physical terms, the ST morphology is most often associated with intervals in which no clear pulse-type or plateau-type signature is observed, and therefore corresponds to a relatively stable local pressure state.

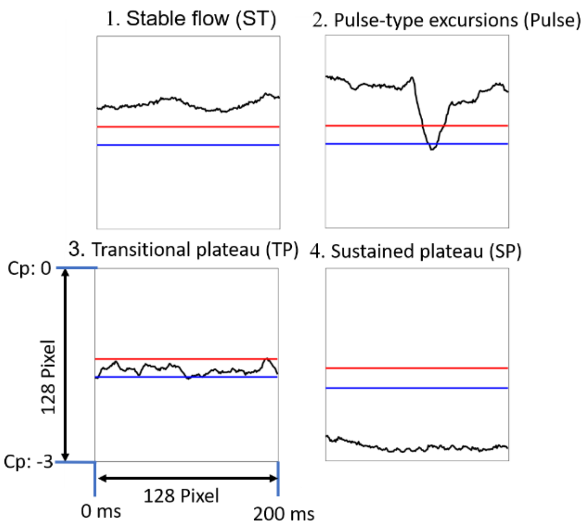

Figure 1. Representative waveform families used in the morphology-based classification framework. Red and blue horizontal lines denote the baseline and depressed-pressure reference levels.

The Pulse family represents impulsive segments characterized by a rapid pressure drop followed by recovery, indicating localized transient disturbances in the near-surface flow. In physical terms, the Pulse morphology is often associated with characteristic-event-like disturbances, namely a rapid pressure drop followed by recovery, as reported by Lai et al. (2023). The TP family corresponds to waveforms exhibiting an emerging low-pressure plateau that is present but not yet temporally persistent, so that the signal retains a transitional character between impulsive and fully developed plateau states. In physical terms, the TP morphology suggests incipient or intermittent development of a low-pressure plateau, and may therefore represent an intermediate state between pulse-type disturbances and a more persistent plateau-type organization.

The SP family represents waveform segments associated with a sustained low-pressure plateau, indicating a more persistent plateau-type pressure organization. In physical terms, the SP morphology suggests a sustained low-pressure organization and is therefore consistent with a more persistent plateau-type state at the measurement location.

These four waveform families should not be interpreted as an exhaustive decomposition of the transitional wake into strictly separated physical modes. Instead, they serve as morphology-based reference classes for organizing the dominant waveform patterns in the pressure data. Their statistical prevalence changes with Reynolds number and measurement location, allowing the present framework to describe regime evolution in a morphology-oriented manner without requiring a strict one-to-one assignment between waveform class and individual flow structure.

Waveform Segmentation and Image Construction

To prepare the pressure signals for morphology-based recognition, each continuous pressure record was divided into fixed 200-ms segments. This window length was selected to preserve sufficient temporal context for each segment to exhibit a recognizable waveform structure while remaining short enough to retain sensitivity to local intermittency and regime variation. In the present Reynolds-number range, the selected window is on the order of two dominant vortex-shedding periods, thereby retaining both short-duration impulsive features and broader waveform organization within a single sample. Each segmented pressure trace was then transformed into a waveform image using a standardized plotting window, as summarized in Figure 3. The vertical axis was fixed to a common pressure-coefficient range from Cp = 0 to Cp = -3.0, while the horizontal axis was fixed by the 200-ms segment duration. The resulting waveform plots were converted into grayscale images with a resolution of 128 × 128 pixels. By embedding all samples in a common visual frame, the classifier evaluates waveform morphology under a consistent pressure and time reference. This preprocessing procedure is not intended to remove all amplitude-related information from the signal. Instead, it preserves waveform morphology within a physically consistent pressure range shared by all samples. As a result, the classifier operates not on arbitrarily normalized traces detached from their pressure context, but on waveform images that retain both shape and pressure-level information under a unified representation. This design is particularly suitable for transitional pressure signals, in which physically meaningful distinctions are often expressed through the combined effects of waveform geometry, persistence, and pressure-depression level.

CNN Classification with Rejection

The waveform images generated from the segmented pressure data were classified using a convolutional neural network (CNN) based on a ResNet50 architecture. Transfer learning was adopted to improve feature-extraction efficiency and to reduce the amount of manually labeled data required for training. The CNN was trained to assign each waveform image to one of the four representative waveform families defined in Figure 1. Through convolution-based feature extraction and hierarchical pattern recognition, the model learns discriminative image features associated with the global morphology of each waveform type.

For each input image, the network outputs a confidence score associated with the predicted class. In the present framework, this confidence measure serves not only as a classification indicator but also as a mechanism for retaining morphologically ambiguous samples. Specifically, if the maximum class confidence is lower than a prescribed threshold, the corresponding segment is not forcibly assigned to any canonical waveform family but is instead labeled as unidentified. This confidence-based rejection step is important because transitional pressure signals frequently contain weakly developed, mixed, or partially transformed patterns that cannot be represented reliably by a strict four-class taxonomy.

The present method therefore differs fundamentally from direct threshold-based event detection. It does not classify waveforms by applying a single numerical cutoff to signal amplitude, duration, or slope. Instead, it evaluates the global morphology of each waveform segment and uses the confidence threshold only as a criterion for classification reliability. For this reason, the framework is more appropriately described as morphology-driven and threshold-reduced, rather than fully determined by the threshold values given. The purpose of the method is not to eliminate all user-defined parameters, but to avoid allowing a single event threshold to dominate the interpretation of complex transitional signals.

Post Hoc Analysis of Unidentified Waveforms

The unidentified category is not treated as a residual error class, but as a physically informative collection of waveform segments that do not conform clearly to the canonical morphology definitions. In transitional flows, intermediate states are expected to arise when the signal exhibits partial development of pulse-like behavior, incomplete plateau formation, weakened sustained plateaus, or mixed signatures produced by the interaction of multiple flow structures. Forcing such segments into one of the canonical waveform families would artificially sharpen the classification boundaries and obscure potentially meaningful transitional behavior.

To further examine the structure of those non-canonical samples, the unidentified waveforms were subjected to post hoc feature-space analysis. After CNN inference, the deep features associated with the unidentified samples were projected into a reduced-dimensional representation, and clustering analysis was performed to determine whether these samples contained recurrent waveform families rather than random outliers. This procedure allows the unidentified group to be reinterpreted as a transitional buffer zone between canonical waveform classes.

The role of this post hoc analysis is therefore twofold. First, it provides a means of testing whether the four canonical waveform families are sufficient to represent the dominant waveform organization over the studied Reynolds-number range. Second, it offers a pathway toward identifying hybrid or weakly developed waveform families that may correspond to physically meaningful intermediate regimes in the evolution of the finite-cylinder wake. Accordingly, the unidentified category should be interpreted not as a failure of the classifier, but as an intentional mechanism for preserving the morphological continuum inherent to transitional pressure signals.

WAVEFORM RECOGNITION PERFORMANCE

Before applying the classification framework to investigate transitional flow organization, the reliability of the CNN-based waveform recognition was evaluated using a labeled dataset of canonical waveform segments. Model performance was evaluated using the F1 score, defined as the harmonic mean of precision and recall. The dataset was divided into training, validation, and testing subsets so that the model performance could be assessed using previously unseen samples. The results show that the CNN can distinguish the four canonical waveform families with high reliability. The overall F1 score reaches approximately 0.94, indicating that the dominant waveform morphologies are captured effectively by the proposed morphology-based framework.

Most misclassifications occur between the TP and SP categories. This is physically reasonable because both classes are plateau-type pressure signatures, and their main difference lies in the persistence and stability of the low-pressure plateau rather than in the presence of an entirely different waveform structure. In contrast, the ST and Pulse categories are generally identified more distinctly because their waveform morphologies differ more clearly from the plateau-related families. Figure 2 presents representative examples of correctly classified waveform images for each category. These examples show that the CNN relies primarily on the overall waveform morphology, including the persistence, recovery behavior, and temporal organization of the signal, rather than on isolated extrema alone. The high classification consistency therefore provides confidence that the proposed framework can be used as a reliable diagnostic tool for examining the statistical organization of pressure-signal states across Reynolds numbers and spanwise locations.

Figure 2. Representative correctly classified waveform images for the four canonical waveform families.

SPANWISE TRANSITION STATISTICS

Figure 3 presents the statistical composition of pressure-signal morphologies identified by the CNN-based classification framework at two representative pressure taps. The morphologies correspond to characteristic waveform patterns in the pressure signals, including ST, Pulse, TP, SP, and unidentified segments.

At the base-level location (Figure 3a, z/D=1, θ=90°), the morphology statistics exhibit a gradual transition as the Reynolds number increases. The pressure signals are initially dominated by the ST morphology. With increasing Reynolds number, pulse-type excursions begin to appear more frequently, followed by a pronounced TP regime where intermittent low-pressure plateaus become dominant. Finally, at higher Reynolds numbers, the statistics become dominated by the SP morphology, indicating the establishment of a persistent low-pressure plateau in the waveform. This multi-stage evolution suggests that the transition near the base proceeds through several intermediate signal states.

A markedly different behavior is observed at the mid-span location (Figure 3b, z/D=2, θ=90°). In this region, the TP fraction is significantly reduced and does not form a distinct regime. Instead, the transition toward SP dominance occurs over a relatively narrow Reynolds-number range. The TP morphology appears only intermittently during this process, indicating that the intermediate signal state is much less pronounced away from the base. The comparison between the two locations indicates that the transition pathway is strongly dependent on the spanwise position along the finite-height cylinder. While the near-base region exhibits a gradual multi-stage transition involving a well-developed TP regime, the mid-span region undergoes a more abrupt transition toward the SP-dominant state.

It should be emphasized that the morphology labels represent pressure-signal patterns identified from the time-series data rather than a strict one-to-one mapping to specific flow structures. Similar waveform morphologies may correspond to different physical mechanisms depending on the local flow state and measurement location. Consequently, the morphology statistics provide a signal-based diagnostic framework for identifying changes in flow behavior, while the detailed physical interpretation must be supported by complementary flow diagnostics such as flow visualization.

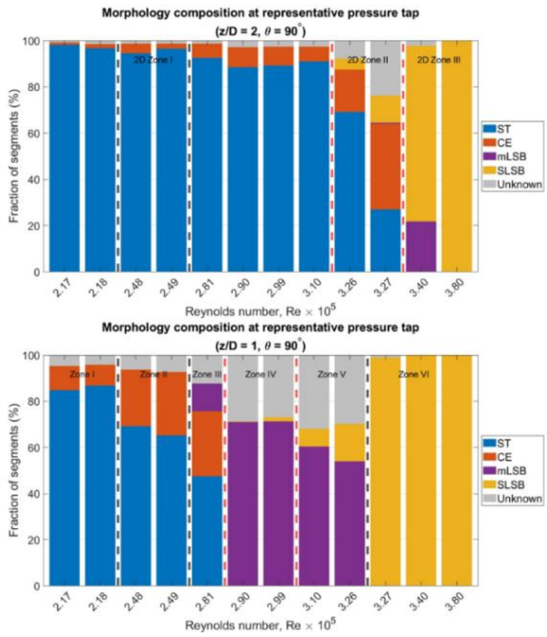

Figure 3. Reynolds-number-dependent waveform composition at two representative pressure taps: (a) z/D = 1, θ = 90°, and (b) z/D = 2, θ = 90°. The results show a clearer multi-stage transition near the base and a more abrupt transition at mid-span.

Based on the morphology statistics shown in Figure 3, the transition process can be broadly divided into several Reynolds-number regimes according to the dominant pressure-signal patterns. At lower Reynolds numbers, the signals are primarily characterized by the ST morphology, indicating a relatively stable flow state without clear evidence of persistent low-pressure plateaus. As the Reynolds number increases, pulse-type excursions become more frequent, marking the onset of intermittent disturbances in the pressure signal. With further increase in Reynolds number, the TP morphology becomes more prominent near the base of the cylinder, representing a transitional regime in which intermittent low-pressure plateaus appear in the pressure waveform. Finally, at higher Reynolds numbers, the SP morphology dominates the signal statistics, indicating the establishment of a persistent low-pressure plateau pattern.

It is noteworthy that the Reynolds-number range associated with each regime varies along the span of the cylinder. Near the base, the TP regime occupies a relatively broad range of Reynolds numbers, whereas at mid-span the transition from ST-dominated behavior to SP dominance occurs more abruptly. This further confirms that the transition dynamics in a finite-height cylinder are strongly influenced by spanwise position. These results demonstrate that the pressure-signal morphology statistics provide a useful framework for identifying transition regimes and reveal strong spanwise variations in the transition process of the finite-height cylinder, with the near-base region exhibiting a clearer multi-stage pathway than the mid-span region.

NON-CANONICAL STATES

To clarify the physical meaning of the samples categorized as Unknown, all Unknown signals were analyzed together in a common feature space constructed from the CNN-extracted deep features. As shown in Figure 4a, these features were projected onto the first two principal components (PC1 and PC2) obtained by principal component analysis (PCA). The projected distribution does not form a diffuse cloud, but instead separates into four major occupied regions, denoted here as C1–C4. The three-dimensional view in Figure 4b further confirms that these four regions remain distinguishable when the third principal component (PC3) is included, indicating that the observed grouping is not merely an artifact of a two-dimensional projection.

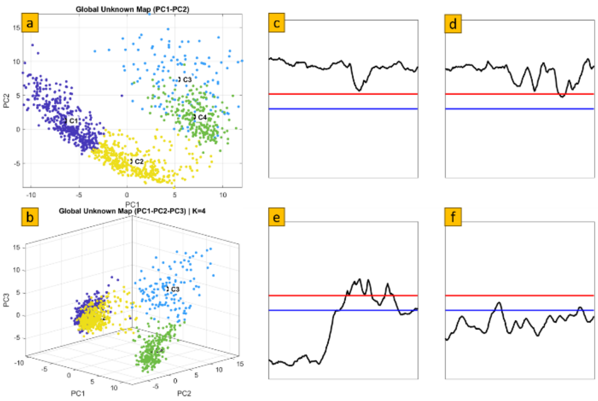

Figure 4. PCA map of Unknown samples: (a) PC1–PC2 projection showing four clusters (C1–C4); (b) PC1–PC3 view confirming their separability; (c–f) representative waveforms for each cluster.

This result suggests that the Unknown class is not simply composed of random outliers or classification failures. Instead, it contains several organized non-canonical branches that are not fully represented by the predefined canonical labels. In other words, although these signals could not be assigned to the standard categories, they still exhibit a structured internal organization in the feature space. The representative waveforms shown in Figure 4(c)–(f) further support this interpretation. Each region is associated with a distinct waveform family. Some signals exhibit weak-event behavior without a clearly developed pressure-recovery plateau, whereas others show more pronounced recovery behavior and stronger oscillatory features. Therefore, the global PCA map indicates that the Unknown samples correspond to physically meaningful non-canonical states rather than residual noise. These states may be interpreted as alternative branches or intermediate forms in the flow evolution that are not sufficiently compact to be absorbed into the canonical classes. Overall, Figure 4a establishes that the Unknown samples occupy four major regions in the global feature space, and that each region is associated with a distinct type of pressure signature. This provides the basis for examining how the occupancy of these non-canonical branches varies with Reynolds number.

A more significant change occurs in the transition regime. In RE025, the Unknown samples spread across all four regions, showing that the transition process cannot be described by a single additional mode. Instead, multiple non-canonical branches coexist simultaneously. Among them, C3 is particularly notable because it becomes prominent mainly in this regime and exhibits the broadest spatial spread in the PCA space. Compared with C1, C2, and C4, the samples in C3 are much less compact, suggesting that this region corresponds to a weakly organized branch, likely associated with transitional, unstable, or intermediate states. This broad distribution is consistent with the idea that C3 represents signals that are difficult to assign to a compact waveform family because they arise during strong mode competition or incomplete development of local flow structures.

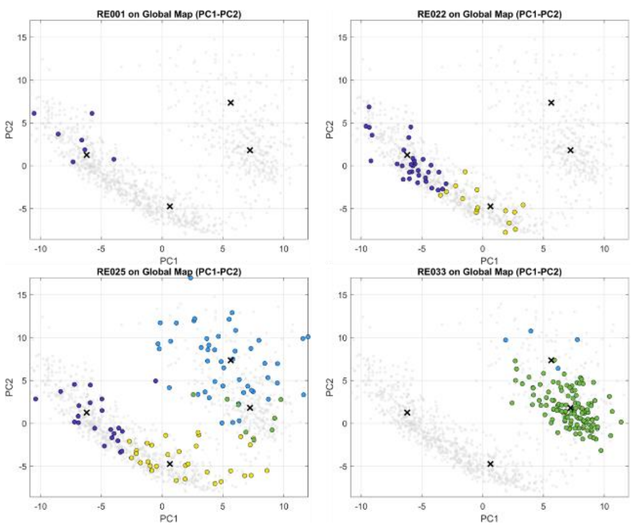

Figure 5. Reynolds-number-dependent occupancy of the four non-canonical regions on the global PCA map.

At higher Reynolds number, represented by RE033, the Unknown samples become concentrated mainly in C4. This indicates that the dominant non-canonical behavior has shifted away from the low-Re C1 branch and the broad transition-related C3 branch toward a more developed high-Re branch. The concentration of samples in C4 suggests that, although these signals remain outside the canonical classes, they are no longer transitional in the same sense as those in C3, but instead correspond to a more established non-canonical state associated with the higher-Re regime. Taken together, Figure 5 reveals a systematic Reynolds-number-dependent evolution of the Unknown states. The dominant occupancy shifts from C1 at low Reynolds number, to the emergence of C2 at intermediate conditions, then broadens into all four regions during transition, with C3 representing the most widely distributed transition-related branch, and finally becomes concentrated in C4 at higher Reynolds number. This progression indicates that the Unknown samples are not random residual events, but structured non-canonical states that evolve with the flow transition process.

CONCLUSIONS

In this study, a morphology-based CNN framework was developed to identify transitional pressure-signal states over a finite circular cylinder in the critical Reynolds-number regime. By converting 200-ms pressure segments into standardized waveform images and classifying them according to their overall morphology, the present method provides a shape-oriented alternative to conventional threshold-dominated event detection. The classification results show that the four canonical waveform families can be recognized with high reliability, with an overall F1 score of approximately 0.94. This demonstrates that the dominant transitional waveform morphologies can be organized effectively through image-based feature extraction and confidence-based classification.

The morphology statistics further reveal that the transition process is strongly spanwise dependent. Near the base part of the cylinder, the signal composition evolves gradually from ST-dominated behavior to pulse-rich activity, followed by a distinct transitional plateau regime and finally a sustained plateau regime. In contrast, the mid-span region shows a much narrower transition range and a less pronounced intermediate stage. These results indicate that the onset and development of transition do not occur uniformly along the finite cylinder, but instead follow a vertically stratified pathway, with the base region entering a more active transitional state earlier than the upper locations, suggesting that proximity to the cylinder base plays an important role in modulating the transition sequence.

A key contribution of the present work is the physical reinterpretation of the Unknown category. Rather than treating unidentified samples as residual classification errors, the post hoc PCA analysis shows that they form four organized regions in the common feature space. Moreover, these regions are populated systematically by different Reynolds-number ranges. The dominant occupancy shifts from C1 at low Reynolds number, to the emergence of C2 at intermediate conditions, then broadens into all four regions during transition, and finally becomes concentrated in C4 at higher Reynolds number. This behavior indicates that the Unknown signals are not random outliers, but structured non-canonical states associated with intermediate, weakly organized, or alternative branches of the transition process.

Overall, the present results suggest that transitional flow over a finite circular cylinder cannot be described adequately by a small set of strictly discrete canonical modes alone. Instead, the flow evolves through both canonical waveform families and a broader continuum of non-canonical states. The proposed morphology-based CNN framework therefore provides not only a practical signal-classification tool, but also a useful framework for examining spanwise transition sequence, intermediate waveform branches, and the structured evolution of non-canonical states in finite-cylinder wakes.

ACKNOWLEDGMENT

Funding support of National Science and Technology Council under the project number: NSTC 114-2221-E-006-132 for this work is very much appreciated.

REFERENCES

Cheng, C., Yang, W., Feng, X., Zhao, Y. and Su, Y. 2024, “A convolutional neural network-based method for distinguishing the flow patterns of gas-liquid two-phase flow in the annulus,” Processes, Vol. 12, pp. 2596.

Kawamura, T., Hiwada, M., Hibino, T., Mabuchi, I. and Kumada, M. 1984, “Flow around a finite circular cylinder on a flat plate: Cylinder height greater than turbulent boundary layer thickness,” Bulletin of JSME, Vol. 27, pp. 2142-2151.

Krajnović, S. 2011, “Flow around a tall finite cylinder explored by large eddy simulation,” Journal of Fluid Mechanics, Vol. 676, pp. 294-317.

Lai, Y.-H. and Miau, J.-J. 2021, “An Investigation into the Nonstationary Characteristics of Separation-Bubble Formation on a Smooth Circular Cylinder in Critical Transition Regime,” Journal of Mechanics, Vol. 37, pp. 415-431.

Lai, Y.-H., Miau, J.-J., Zhung, G.-T., Tsai, M.-C. and Wu, J.-C. 2023, “Characteristics of Separation-Bubble Formation on Finite Circular Cylinder in Critical Transition Range,” AIAA journal, Vol. 61, pp. 4468-4484.

Ni, C., Charoenphakdee, N., Honda, J. and Sugiyama, M. 2019, “On the calibration of multiclass classification with rejection,” Advances in neural information processing systems, Vol. 32.

Sumner, D. 2013, “Flow above the free end of a surface-mounted finite-height circular cylinder: A review,” Journal of Fluids and Structures, Vol. 43, pp. 41-63.

Veerasamy, D. and Atkin, C. 2020, “A rational method for determining intermittency in the transitional boundary layer,” Experiments in Fluids, Vol. 61, pp. 11.

Wen, S., Lee, M. W., Bastos, K. M. K., Eldridge-Allegra, I. K. and Dowell, E. H. 2023, “Feature identification in complex fluid flows by convolutional neural networks,” Theoretical and Applied Mechanics Letters, Vol. 13, pp. 100482.

Zhang, D., Chew, Y. and Winoto, S. 1996, “Investigation of intermittency measurement methods for transitional boundary layer flows,” Experimental Thermal and Fluid science, Vol. 12, pp. 433-443.